

VideoFusion: Decomposed Diffusion Models for High-Quality Video Generation

*Zhengxiong Luo^{1,2,4,5} Dayou Chen² Yingya Zhang²

†Yan Huang^{4,5} Liang Wang^{4,5} Yujun Shen³ Deli Zhao² Jingren Zhou² Tieniu Tan^{4,5,6}

¹University of Chinese Academy of Sciences (UCAS) ²Alibaba Group

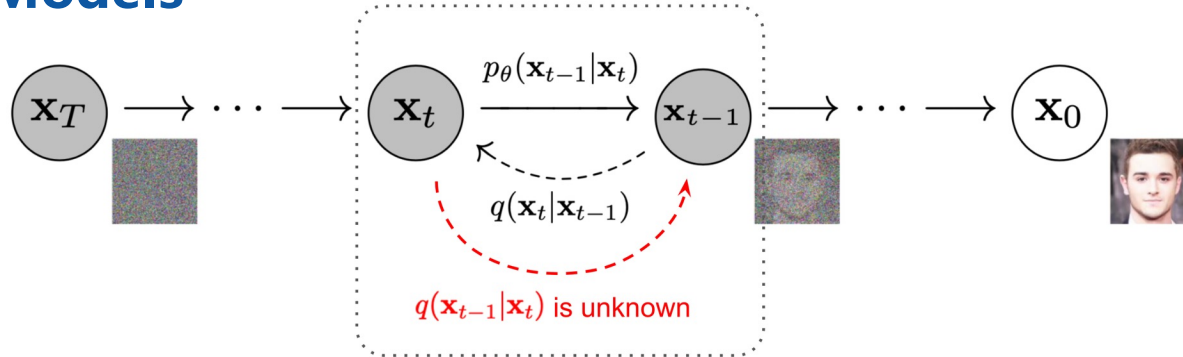
³Ant Group ⁴Center for Research on Intelligent Perception and Computing (CRIPAC)

⁵Institute of Automation, Chinese Academy of Sciences (CASIA) ⁶Nanjing University

*Work done at Alibaba DAMO Academy.

†Corresponding author.

| Diffusion Models



- Encoding:

$$x_t = \sqrt{1 - \beta_t} x_{t-1} + \sqrt{\beta_t} \epsilon_{t-1}$$

$$s.t. \quad \epsilon_{t-1} \sim N(0, 1)$$

$$p(x_t|x_{t-1}) \sim N(\sqrt{1 - \beta_t} x_{t-1}, \beta_t)$$

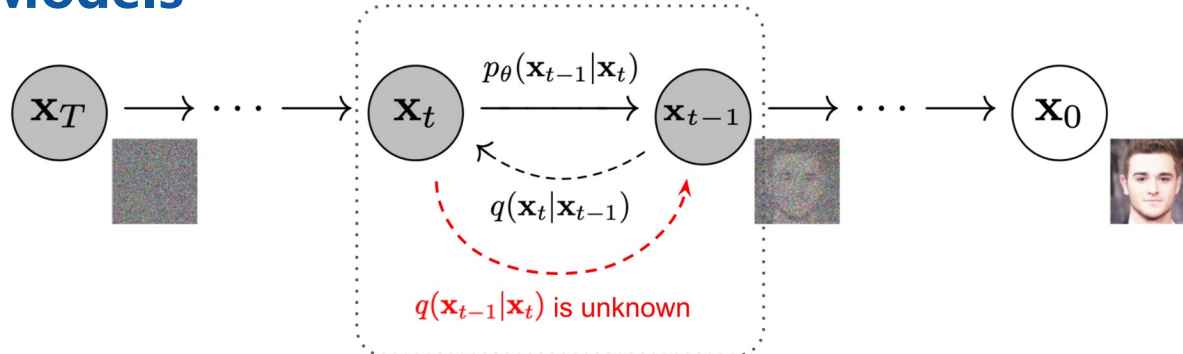


$$x_t = \sqrt{\hat{\alpha}_t} x_0 + \sqrt{1 - \hat{\alpha}_t} \hat{\epsilon}_t$$

$$s.t. \quad \left\{ \begin{array}{l} \hat{\alpha}_t = \prod_{t=1}^T \alpha_t \\ \hat{\epsilon}_t \sim N(0, 1) \\ \alpha_t = 1 - \beta_t \end{array} \right.$$

$$p(x_t|x_0) \sim N(\sqrt{\hat{\alpha}_t} x_0, 1 - \hat{\alpha}_t)$$

| Diffusion Models



- Decoding:

$$\begin{aligned} q(x_{t-1}, x_t | x_0) &= q(x_{t-1} | x_t, x_0)q(x_t | x_0) \\ &= q(x_t | x_{t-1}, x_0)q(x_{t-1} | x_0) \end{aligned} \quad \longrightarrow \quad q(x_{t-1} | x_t, x_0) = \frac{q(x_t | x_{t-1}, x_0)q(x_t | x_0)}{q(x_{t-1} | x_0)}$$

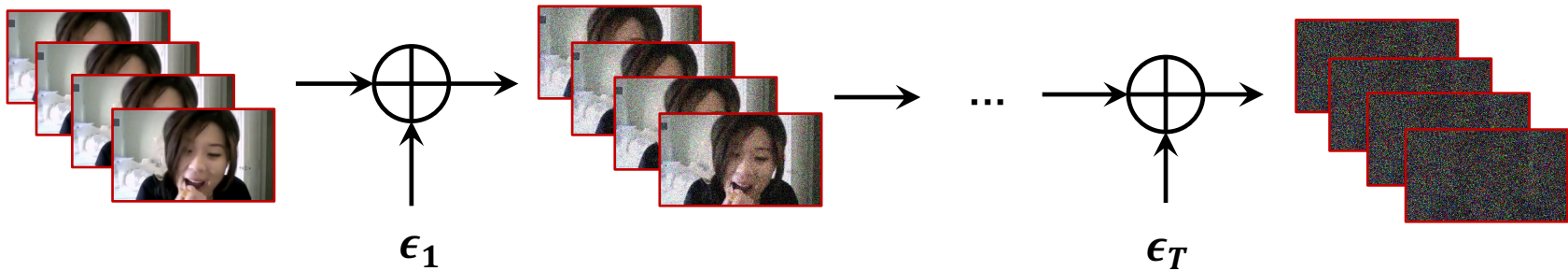
$$\longrightarrow x_{t-1} = \frac{x_t}{\sqrt{\alpha_t}} - \frac{\sqrt{1-\alpha_t}}{\sqrt{\alpha_t}} \sqrt{1-\eta} z_\theta - \frac{\sqrt{1-\alpha_t}}{\sqrt{\alpha_t}} \sqrt{\eta} \epsilon'_t \quad s.t. \quad \begin{cases} \hat{\epsilon}_t := z_\theta(\mathbf{x}_t, t) \\ \epsilon'_t \sim N(0, 1) \end{cases}$$

$\eta = 0 \rightarrow$ DDIM Sampling

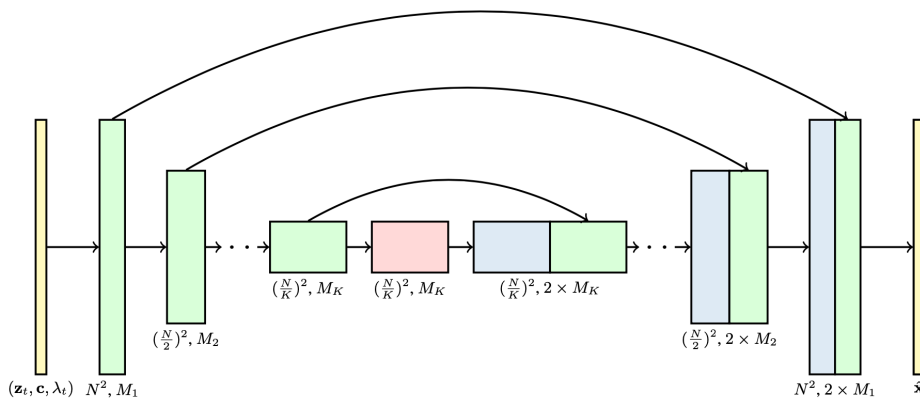
$\eta = \frac{1 - \hat{\alpha}_{t-1}}{1 - \hat{\alpha}_t} \alpha_t \rightarrow$ DDPM Sampling

Related Works

- Encoding:



- Decoding:



- Each frame is **individually encoded**, ignoring the temporal correlation and redundancy.
- The coherence of the generated videos **relies only on the temporal attention module** in the denoising network.

I Decomposed Diffusion Models

$$x^i = \sqrt{\lambda^i}x^0 + \sqrt{1 - \lambda^i}\Delta x^i, \quad i = 1, 2, \dots, N$$

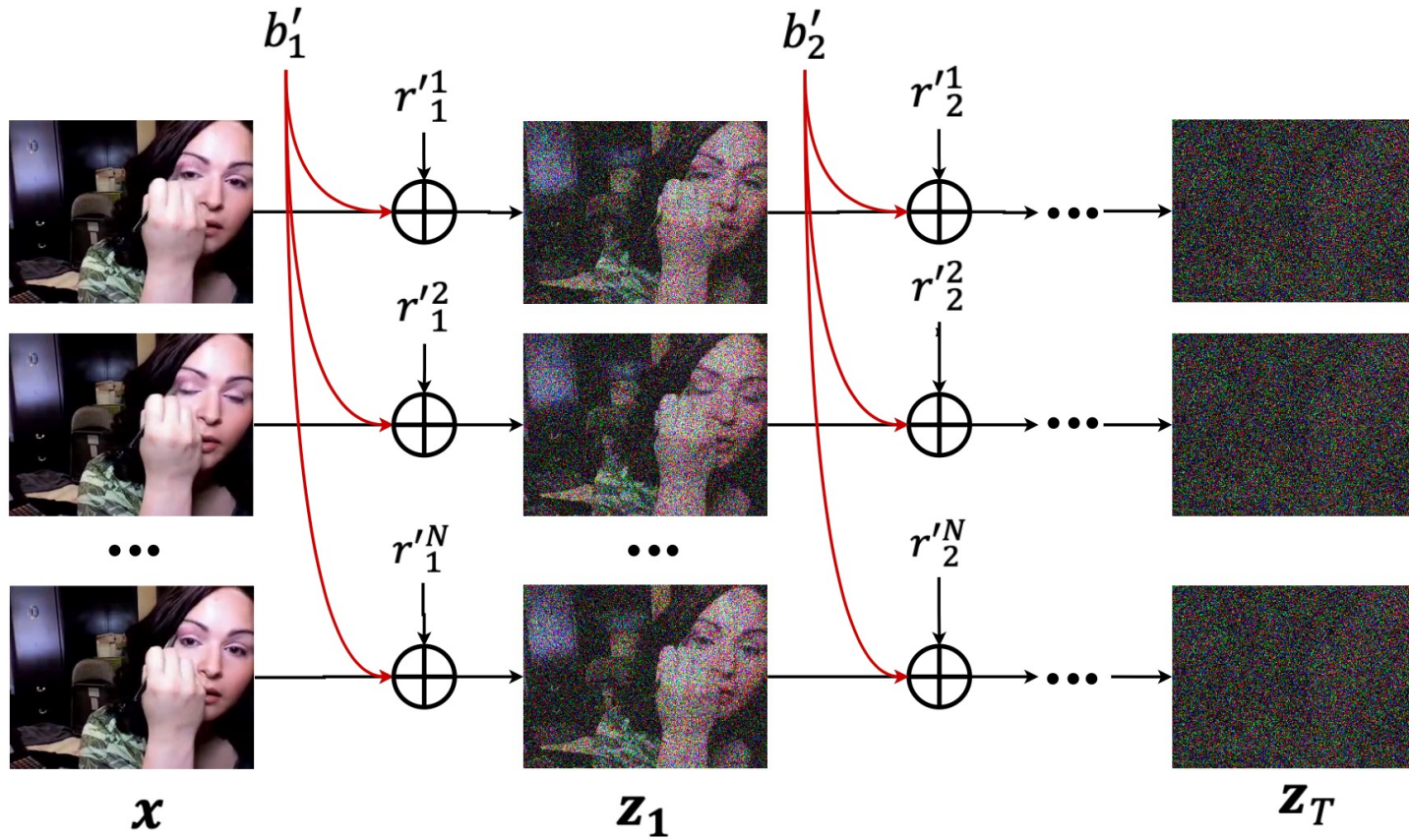
$$\downarrow$$
$$z_t^i = \sqrt{\hat{\alpha}_t}(\sqrt{\lambda^i}x^0 + \sqrt{1 - \lambda^i}\Delta x^i) + \sqrt{1 - \hat{\alpha}_t}\epsilon_t^i$$

$$\downarrow$$
$$\epsilon_t^i = \sqrt{\lambda^i}b_t^i + \sqrt{1 - \lambda^i}r_t^i \quad b_t^i, r_t^i \sim \mathcal{N}(0, 1)$$

$$\downarrow$$
$$z_t^i = \underbrace{\sqrt{\lambda^i}(\sqrt{\hat{\alpha}_t}x^0 + \sqrt{1 - \hat{\alpha}_t}b_t^i)}_{\text{diffusion of } x^0} +$$

$$\underbrace{\sqrt{1 - \lambda^i}(\sqrt{\hat{\alpha}_t}\Delta x^i + \sqrt{1 - \hat{\alpha}_t}r_t^i)}_{\text{diffusion of } \Delta x^i}.$$

I Decomposed Diffusion Models



| Decomposed Diffusion Models



Figure 2. Comparisons between images generated from (a) independent noises; (b) noises with a shared base noise. Images of the same row are generated by the decoder of DALLE-2 [24] with the same condition.

I Decomposed Diffusion Models

$$z_t^i =$$

$$\begin{cases} \sqrt{\hat{\alpha}_t}x^i + \sqrt{1 - \hat{\alpha}_t}b_t & i = \lfloor N/2 \rfloor \\ \sqrt{\hat{\alpha}_t}x^i + \sqrt{1 - \hat{\alpha}_t}(\sqrt{\lambda^i}b_t + \sqrt{1 - \lambda^i}r_t^i) & i \neq \lfloor N/2 \rfloor \end{cases}$$

$$\mathcal{L}_t =$$

$$\begin{cases} \|\epsilon_t^i - \mathbf{z}_\phi^b(z_t^{\lfloor N/2 \rfloor}, t)\|^2 & i = \lfloor N/2 \rfloor \\ \|\epsilon_t^i - \sqrt{\lambda^i}[\mathbf{z}_\theta^b(z_t^{\lfloor N/2 \rfloor}, t)]_{sg} - \sqrt{1 - \lambda^i}\mathbf{z}_\psi^r(z_t'^i, t, i)\|^2 & i \neq \lfloor N/2 \rfloor \end{cases}$$

$$\begin{cases} \|\epsilon_t^i - \mathbf{z}_\phi^b(z_t^{\lfloor N/2 \rfloor}, t)\|^2 & i = \lfloor N/2 \rfloor \\ \|\epsilon_t^i - \sqrt{\lambda^i}[\mathbf{z}_\theta^b(z_t^{\lfloor N/2 \rfloor}, t)]_{sg} - \sqrt{1 - \lambda^i}\mathbf{z}_\psi^r(z_t'^i, t, i)\|^2 & i \neq \lfloor N/2 \rfloor \end{cases}$$

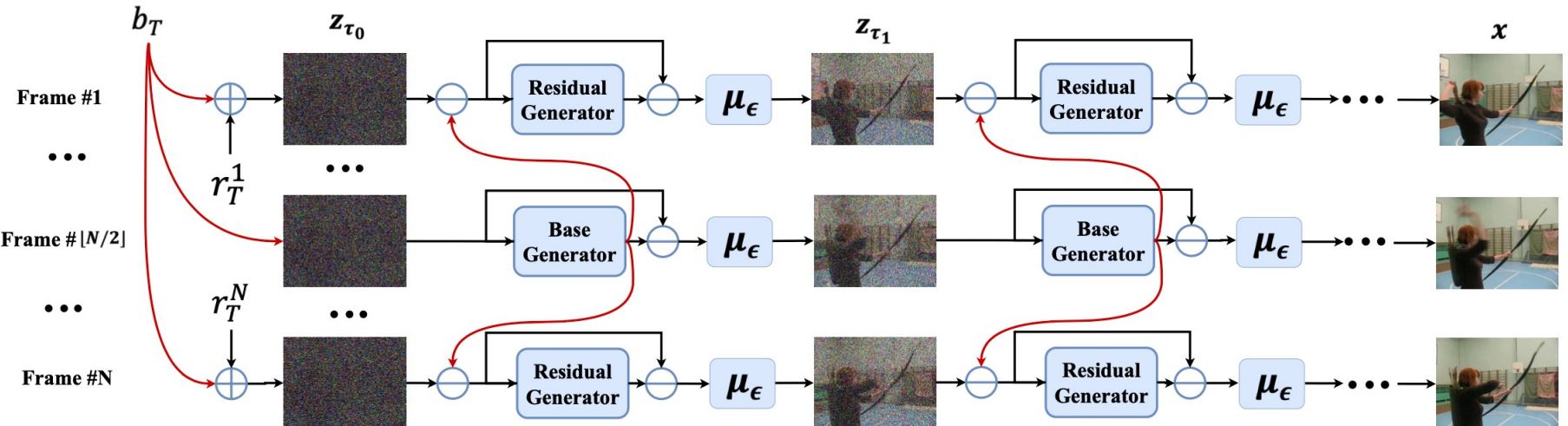


Figure 4. Visualization of DDIM [35] sampling process of DecDPM. In each sampling step, we first remove the base noise with the base generator and then estimate the remaining residual noise via the residual generator. τ_i denotes the DDIM sampling steps. μ_ϵ denotes mean-value predicted function of DDIM in ϵ -prediction formulation. We omit the coefficients and conditions in the figure for simplicity.

Decomposed Diffusion Models

Algorithm 2 DDIM Sampling

Sampling $b \sim \mathcal{N}(0, 1)$, $z^{\lfloor N/2 \rfloor} \leftarrow b$
 for $i = 1$ to N and $i \neq \lfloor N/2 \rfloor$ do
 Sampling $r^i \sim \mathcal{N}(0, 1)$

$$z^i = \sqrt{\lambda^i}b + \sqrt{1 - \lambda^i}r^i$$

 end for
 for $t = T$ to 1 do

$$b \leftarrow \mathbf{z}_\phi^b(z^{\lfloor N/2 \rfloor}, t); \epsilon^{\lfloor N/2 \rfloor} \leftarrow b$$

 for $i = 1$ to N and $i \neq \lfloor N/2 \rfloor$ do

$$z'^i \leftarrow z^i - \sqrt{\lambda^i}\sqrt{1 - \hat{\alpha}b}$$

$$r^i \leftarrow \mathbf{z}_\psi^r(z'^i, t, i)$$

$$\epsilon^i \leftarrow \sqrt{\lambda^i}b + \sqrt{1 - \lambda^i}r^i$$

 end for
 for $i = 1$ to N do

$$z^i \leftarrow \sqrt{\hat{\alpha}_{t-1}}\left(\frac{z^i - \sqrt{1 - \hat{\alpha}_t}\epsilon^i}{\sqrt{\hat{\alpha}_t}}\right) + \sqrt{1 - \hat{\alpha}_{t-1}}\epsilon^i$$

 end for
 end for
 return $\{z^i \mid i = 1, 2, \dots, N\}$

Algorithm 1 DDPM Sampling

Sampling $b \sim \mathcal{N}(0, 1)$, $z^{\lfloor N/2 \rfloor} \leftarrow b$
for $i = 1$ to N **and** $i \neq \lfloor N/2 \rfloor$ **do**
 Sampling $r^i \sim \mathcal{N}(0, 1)$

$$z^i = \sqrt{\lambda^i}b + \sqrt{1 - \lambda^i}r^i$$

end for
for $t = T$ to 1 **do**

$$b \leftarrow \mathbf{z}_\phi^b(z^{\lfloor N/2 \rfloor}, t); \epsilon^{\lfloor N/2 \rfloor} \leftarrow b$$

for $i = 1$ to N **and** $i \neq \lfloor N/2 \rfloor$ **do**

$$z'^i \leftarrow z^i - \sqrt{\lambda^i}\sqrt{1 - \hat{\alpha}b}; r^i \leftarrow \mathbf{z}_\psi^r(z'^i, t, i)$$

$$\epsilon^i \leftarrow \sqrt{\lambda^i}b + \sqrt{1 - \lambda^i}r^i$$

end for
for $i = 1$ to N **do**

$$\mu^i \leftarrow \frac{1}{\sqrt{\alpha_t}}z^i - \frac{1 - \alpha_t}{\sqrt{1 - \hat{\alpha}_t}\sqrt{\alpha_t}}\epsilon^i; \sigma \leftarrow \frac{1 - \hat{\alpha}_{t-1}}{1 - \hat{\alpha}_t}(1 - \alpha_t)$$

end for
 Sampling $b \sim \mathcal{N}(0, 1)$

$$z^{\lfloor N/2 \rfloor} \leftarrow \sigma b + \mu^{\lfloor N/2 \rfloor}$$

for $i = 1$ to N **and** $i \neq \lfloor N/2 \rfloor$ **do**
 Sampling $r^i \sim \mathcal{N}(0, 1)$

$$z^i \leftarrow \sigma(\sqrt{\lambda^i}b + \sqrt{1 - \lambda^i}r^i) + \mu^i$$

end for
end for
 return $\{z^i \mid i = 1, 2, \dots, N\}$

Experiments

Table 1. Quantitative comparisons on UCF101. \downarrow denotes the lower the better. \uparrow denotes the higher the better. The best results are denoted in bold.

Method	Resolution	IS \uparrow	FVD \downarrow
<i>Unconditional</i>			
TGAN [29]	$16 \times 64 \times 64$	11.85	—
MoCoGAN-HD [40]	$16 \times 128 \times 128$	32.36	838
DIGAN [50]	$16 \times 128 \times 128$	32.70	577
StyleGAN-V [34]	$16 \times 256 \times 256$	23.94	—
VideoGPT [47]	$16 \times 128 \times 128$	24.69	—
TATS [9]	$16 \times 128 \times 128$	57.63	420
VDM [16]	$16 \times 64 \times 64$	57.00	295
VideoFusion	$16 \times 64 \times 64$	71.67	139
VideoFusion	$16 \times 128 \times 128$	72.22	220
<i>Class-conditioned</i>			
VGAN [45]	$16 \times 64 \times 64$	8.31	—
TGAN [29]	$16 \times 64 \times 64$	15.83	—
TGANv2 [30]	$16 \times 128 \times 128$	28.87	1209
MoCoGAN [40]	$16 \times 64 \times 64$	12.42	—
DVD-GAN [4]	$16 \times 128 \times 128$	32.97	—
CogVideo [17]	$16 \times 160 \times 160$	50.46	626
TATS [9]	$16 \times 128 \times 128$	79.28	332
VideoFusion	$16 \times 128 \times 128$	80.03	173

Table 2. Quantitative comparisons on Sky Time-lapse [46]. \downarrow denotes the lower the better. The best results are denoted in bold.

Method	FVD (\downarrow)	KVD (\downarrow)
MoCoGAN-HD [40]	183.6	13.9
DIGAN [50]	114.6	6.8
TATS [9]	132.6	5.7
VideoFusion	47.0	5.3

Table 3. Quantitative comparisons on TaiChi-HD [33]. \downarrow denotes the lower the better. The best results are denoted in bold.

Method	FVD (\downarrow)	KVD (\downarrow)
MoCoGAN-HD [40]	144.7	25.4
DIGAN [50]	128.1	20.6
TATS [9]	94.6	9.8
VideoFusion	56.4	6.9

I Experiments

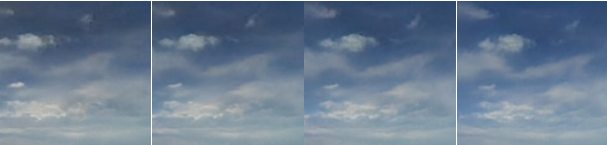
TATS



DIGAN



VideoFusion



(a) UCF101

(b) Sky Time-Lapse

(c) TaiChi-HD

Experiments

Table 4. We re-implement VDM [16] (denoted as VDM*) based on the base generator of VideoFusion. The efficiency comparisons are shown below.

Method	Memory (GB)	Latency (s)
VDM*	63.82	0.40
VideoFusion	49.85(\downarrow 21.8%)	0.17(\downarrow 57.5%)

Table 5. Study on λ^i . Unconditional generation results on UCF101 [39].

λ^i	0.10	0.25	0.50	0.75
IS \uparrow	67.23	69.16	71.67	69.56
FVD \downarrow	149	122	139	181

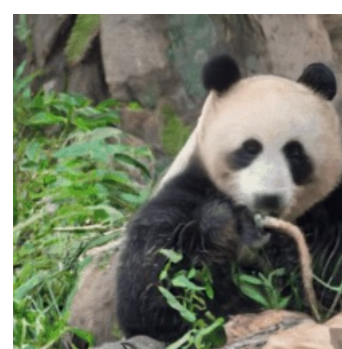
Table 6. Study on pretraining. Unconditional generation results on UCF101 [39].

Method	IS \uparrow	FVD \downarrow
VDM [16]	57.00	295
VideoFusion w/o pretrain	65.29	183
VideoFusion w/ pretrain	71.67	139

Table 7. Study on joint training. Unconditional generation results on UCF101 [39].

Training method	IS \uparrow	FVD \downarrow
Fixed	65.06	187
w/o stop gradient	67.86	168
w stop gradient	71.67	139

I Experiments Results



I Experiments Results

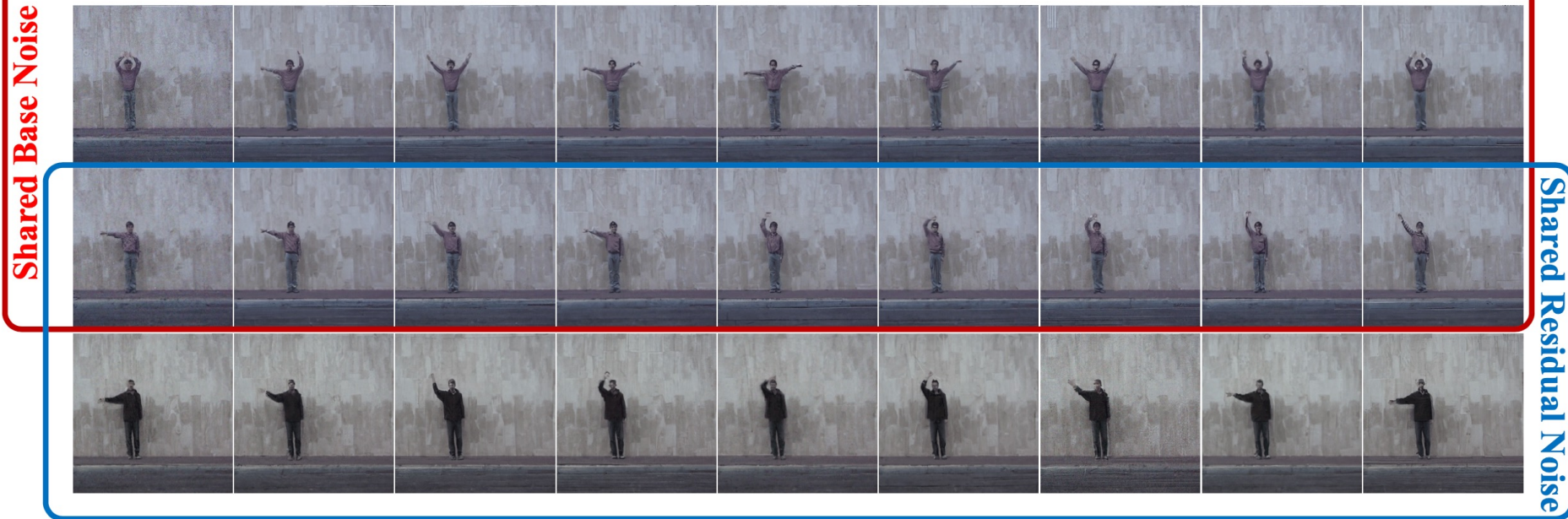


Figure 1. Unconditional generation results on the Weizmann Action datasets [11]. Videos of the top-two rows share the same base noise but have different residual noises. Videos of the bottom-two rows share the same residual noise but have different base noises.

Additional Information

https://www.modelscope.cn/models/damo/cv_diffusion_text-to-video-synthesis/summary

模型库 / cv_diffusion_text-to-video-synthesis

通义-文本生成视频大模型-英文-通用领域-v1.0 集成中

damo/cv_diffusion_text-to-video-synthesis (达摩院 提供 | 52 次下载)

文本生成视频 PyTorch 开源协议: CC-BY-NC-ND text2video generation diffusion model 文到视频 文生视频 文本生成视频 生成

模型介绍

模型文件

快速使用

提交反馈

论坛交流

<https://www.modelscope.cn/models/damo/text-to-video-synthesis/summary>

模型库 / text-to-video-synthesis

文本生成视频大模型-英文-通用领域

damo/text-to-video-synthesis (达摩院 提供 | 24037 次下载)

文本生成视频 PyTorch 开源协议: CC-BY-NC-ND text2video generation diffusion model 文到视频 文生视频 文本生成视频 生成

模型介绍

模型文件

快速使用

提交反馈

论坛交流

Q&A